Scraping and Stapling of End-Grafted DNA Chains by a Bioadhesive Spreading Vesicle to Reveal Chain Internal Friction and Topological Complexity

Gimoon Nam,[1,2] Marie Laure Hisette,[2] Yuting Liang Sun,[2] Thomas Gisler,[3] Albert Johner,[2] Fabrice Thalmann,[2] André Pierre Schröder,[2] Carlos Manuel Marques,[2,*] and Nam-Kyung Lee[1,†]

[1]*Institute of Fundamental Physics, Department of Physics, Sejong University, Seoul 143-743, Korea*
[2]*Institut Charles Sadron, Université de Strasbourg, CNRS UP22 67034, Strasbourg cedex 2, France*
[3]*Fachbereich Physik, Universiät Konstanz, Fach M621, Konstanz, 78457, Germany*

(Received 17 February 2010; published 17 August 2010)

Stained end-grafted DNA molecules about 20 μm long are scraped away and stretched out by the spreading front of a bioadhesive vesicle. Tethered biotin ligands bind the vesicle bilayer to a streptavidin substrate, stapling the DNAs into frozen confinement paths. Image analysis of the stapled DNA gives access, within optical resolution, to the local stretching values of individual DNA molecules swept by the spreading front, and provides evidence of self-entanglements.

DOI: 10.1103/PhysRevLett.105.088101 PACS numbers: 87.15.−v, 36.20.Ey, 82.70.Uv

It has been recently shown [1] that when a bioadhesive phospholipid vesicle is brought into contact with a carpeted surface of end-grafted λ-phage DNA, the spreading front of the adhesive patch [2] propagates outwards from a nucleation center, acting as a scraper that strongly stretches the DNA chains. Moreover, the multiple bonds created during vesicle spreading effectively staple the stretched chains in the gap between the membrane and the substrate, confining the DNA chains in a tunnel-like channel as depicted in Fig. 1. The chain configuration starts thus at its fixed, end-grafted point at the streptavidin substrate. This surface-attached protein layer of receptors strongly binds the tethered biotin ligands carried by some of the bilayer phospholipids. From its grafted end, the chain meanders through the forest of short polymer tethers that connect the phospholipid membrane above the chain to the protein bed below it, eventually exiting the adhesive gap to adopt a coil-like configuration in the corner between the almost vertical vesicle wall and the horizontal protein surface. We show in this Letter that such an experimental geometry provides not only a unique tool for studying single DNA stretching and confinement in a biomimetic environment, but it also reveals the internal friction and the topological complexity of the DNA chains.

Experimental methods and materials were described elsewhere [1]. Briefly, the vesicles are prepared by electroformation, from a mixture of two lipids (Avanti Polar Lipids): 1,2-dioleoyl-sn-glycero-3-phosphocholine (DOPC) and 1,2-distearoyl-sn-glycero-3-phosphoethanolamine-*N*-[biotinyl(polyethylene-glycol) 2000] (DSPE-PEG2000-biotin) in different ratios. The biotinilated lipids allow the vesicles to strongly bind to a glass substrate covered with streptavidin, which also anchor biotinilated λ-phage DNA, with average end-grafting density of $1/(5\ \mu\text{m}^2)$, well below the surface overlapping concentration. The conformations of the individual grafted DNA molecules were observed by fluorescence microscopy, the λ DNA being stained with YOYO-1 (Molecular Probes), as shown in Figs. 1 and 2. The localization and extension of the adhesive patch were determined by reflection interference contrast microscopy (RICM); see Fig. 1. A typical DNA image consists of a bright head part located outside the adhesive patch region and a tail located inside. The whole conformation can also be located under the adhered membrane without a bright head. We distinguish

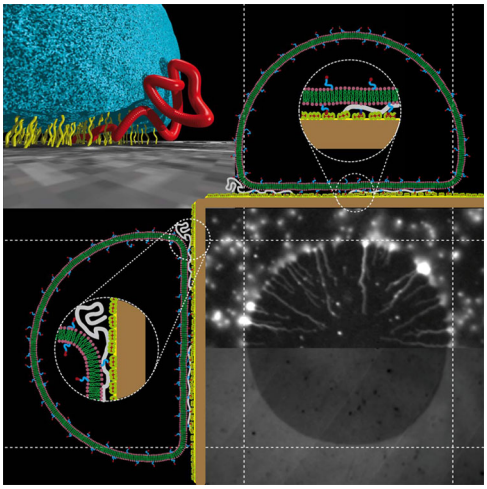

FIG. 1 (color online). The top left image shows schematically the confinement geometry of the DNAs analyzed in this Letter. A phospholipid giant unilamellar vesicle is attached to a substrate by short polymer anchors. The spreading of this attachment region scrapes the end-grafted DNA molecule, stretching and stapling it between the membrane and the substrate as the adhesion front advances. The bottom right image combines in a Janus display (i) a typical optical fluorescence image where the stretched DNAs are seen as bright lines and the coiled DNA regions as bright light spots and (ii) a typical RICM image where the adhesion patch appears as a darker disk. The bottom left and top right drawings further show typical features of the confined geometry.

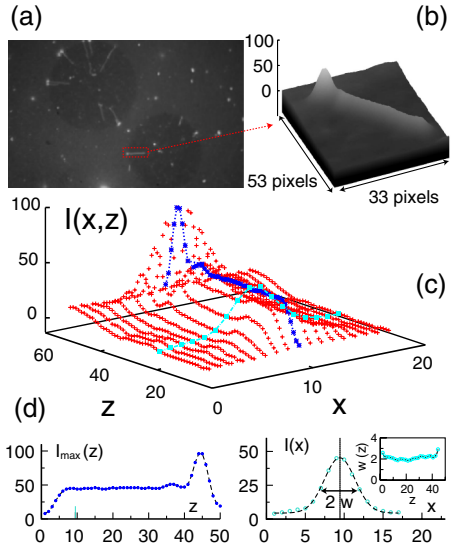

FIG. 2 (color online). (a) A typical DNA fluorescence image and (b) a 3D intensity representation of a single DNA cropped from the image. (c) The cross-sectional areas are fit with Gaussian distribution, and the peak of each Gaussian distribution is marked by dark blue star. (d) Intensity profiles of a single DNA image along the longitudinal direction (left) and cross-sectional distribution (right).

between headed and nonheaded conformations and name them *tadpoles* and *tapeworms*, respectively; see Fig. 3. Conformational relaxation is never observed throughout the experimental time; DNA configurations remain as produced by the spreading and stapling process.

Figure 2 illustrates the conformational analysis performed from each DNA fluorescence image. The pixel size corresponds to 0.18 μm; thus, fully stretched λ-phage DNA with contour length $S = 19.8$ μm would span 110 pixels [3]. Since one phospholipid occupies a cross-sectional area of 0.75 nm^2, a fraction n of biotinilated phospholipids corresponds to a ligand surface density $\sigma = 1.33n$ nm^{-2}. We have analyzed over 200 images of DNA obtained for various values of ligand fractions $n = 1/25$, $1/50$, $1/500$, and $1/5000$ corresponding, respectively, to $\sigma = 5.33 \times 10^{-2}$, 2.66×10^{-2}, 2.66×10^{-3}, and 2.66×10^{-4} nm^{-2}. After extracting a single DNA image from the fluorescence images, we first subtract the gray level of the background to obtain three-dimensional representations of the intensity as shown in Fig. 2(b). After rotation each DNA image provides the intensity distribution $I(x, z)$ as displayed in Fig. 2(c). The cross-sectional distribution, i.e., the distribution in the direction orthogonal to z, is measured to be Gaussian. For most tailed configurations the width of the Gaussian distribution $w(z)$ is almost constant along the z direction, as shown in the inset of Fig. 2(d), and the height of the distribution $I_{\max}(z)$ is hence proportional to the cross-sectional intensity. The height of the intensity profile $I_{\max}(z)$ along the z direction is shown in Fig. 2(d) together with a typical Gaussian cross section.

Assuming an homogeneous random distribution of fluorophores along the DNA backbone, one expects the intensity of each pixel $I(x, z)$ to be proportional to the DNA length it stores. After normalization with the total intensity $I_t = \sum_{x,z} I(x, z)$ of monodisperse DNAs, the reduced intensity $i(x, z) = I(x, z)/I_t$ can be interpreted as the fraction of the DNA segments located in the pixel. The normalized cross-sectional intensity $m(z) = [\sum_x i(x, z)] \times$ (DNA contour length in pixels) $- 1$, measured at a distance z away from the grafting position, gives the relative excess length of DNA along z, a value of $m = 0$ corresponding to fully stretched DNA.

The insets in Fig. 3 exhibit conformations and typical profiles of the relative excess length $m(z)$ for tadpoles and tapeworms at ligand fractions $n = 1/50$ corresponding to an obstacle density $\sigma = 2.66 \times 10^{-2}$ nm^{-2}. As expected for tadpoles, the m values are sharply peaked at the edge of

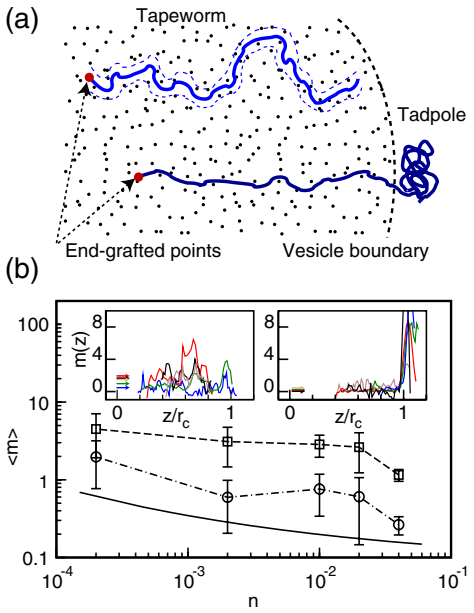

FIG. 3 (color online). (a) Illustration of the conformations of a tapeworm, a DNA chain fully confined below the membrane, and a tadpole, a DNA chain having only a fraction of its length, the tail, confined below the membrane, while the rest of the chain, the head, is in a coiled configuration outside the adhesive patch. (b) Typical profiles of the relative excess length $m(z)$ of tapeworms and tadpoles are shown, respectively, in the left and right insets at ligand fraction $n = 1/50$. The average values $\bar{m}$ of the plateau heights are there indicated by arrows, and z is rescaled by the membrane radius r_c. The curves in the figure show $\langle m \rangle$, an average of $\bar{m}$ values of up to ten chains, as a function of the ligand fraction n for (i) tapeworms (dashed line) and (ii) tadpoles (dot-dashed line). The continuous line shows theoretical predictions for semiflexible chains in a confinement tunnel. [See Eq. (1) and text thereafter.] Clearly, confinement effects alone cannot explain the data, demonstrating the existence of a longer suboptical primitive path for the confining tunnel.

the membrane due to the fluctuating coil. The confined part of a tadpole, the tail, has small $m(z)$ values and is hence stretched. Significantly, tapeworms are less stretched than tadpoles and exhibit a much larger dispersion in stretching values. The mean plateau height $\bar{m}$ for each DNA is defined for each intensity profile. For various values of ligand fractions n, we obtained mean values $\langle m \rangle$ by averaging plateau heights $\bar{m}$ of up to 10 chains. Figure 3 shows dependence of $\langle m \rangle$ on the binder's density n for both tapeworms and tadpoles, providing a quantitative measure for the differences in stretching between both configurations. We also measured mean-square average values $\langle \delta m^2 \rangle = \langle (m(z) - \bar{m})^2 \rangle$ by averaging first over the chain extension and then over different chains. Standard deviations $\langle \delta m^2 \rangle^{1/2}$ range for the tadpoles from 0.4 at the highest ligand densities to 0.7 for the lowest, while the corresponding tapeworm values are roughly twice as large in the corresponding range [0.7–1.3]. We now compare results from our local conformational analysis with theoretical predictions for confined semiflexible wormlike chains.

The scraping and stapling process stretches the DNA and freezes in its tunnel primitive path, that is the two-dimensional (z, x) shape of the tunnel confining the chain. In the vertical direction y the tunnel size is determined by the distance h between the membrane and the substrate, with roughly $h \simeq 10$ nm as estimated from RICM. In the direction x parallel to the plane, the tunnel size d is defined by the distance between multiple bonds connecting the membrane to the substrate $d \simeq \sigma^{-1/2} = 0.9 n^{-1/2}$ nm. One has $d \simeq 5$ nm for the densest binding with $n = 1/25$ and $d \simeq 60$ nm for the loosest with $n = 1/5000$. At the end of the spreading process the chain can relax within its tunnel where it is still expected to display confined thermal fluctuations. Given the suboptical nature of the tunnel dimensions h and d, such thermally induced fluctuations, easily seen in the coil head of the tadpoles, cannot be observed neither for the tapeworms nor for the tail sections of the tadpoles. Also, escape from the primitive path tunnels was never observed, consistent with typical distances d between binders smaller than the DNA persistence length $\ell_p \simeq 70$ nm, $0.07 < d/\ell_p < 0.90$. Note that the shape of the tunnel primitive path can only be experimentally determined up to the optical resolution; significant undulations can still be present even within a frozen, optically straight path. Confined thermal fluctuations and suboptical waviness of the primitive path thus provide two possible sources for accounting for the DNA length storage measured by the $m > 0$ values of the relative excess length. Small local entanglements resilient to unwinding during scraping provide a third possible storage source for the relative excess length that we will extensively discuss below.

The conformations of semiflexible chains of length S, with persistence length l_p under a force f, confined inside of a tube with section dimensions $(h, d) \ll \ell_p$ can be computed from the Hamiltonian $H = S\sum_q (k_B T \ell_p q^4 + f q^2 + B_x) x_q x_{-q}/2 + S\sum_q (k_B T \ell_p q^4 + f q^2 + B_y) y_q y_{-q}/2$ where the chain is described by the parametric representation $x(z)$, $y(z)$ and its Fourier transforms x_q, y_q. Fixing the amplitudes B_x, B_y of the confinement potential by requiring zero force mean-square amplitudes $\langle x^2 \rangle = d^2$ and $\langle y^2 \rangle = h^2$, one gets the average of the relative excess length

$$1 - \frac{\langle L \rangle}{S} = \frac{1}{4}\left(\left[\frac{\ell_p}{d}\right]^{4/3} + \tilde{f}\right)^{-1/2} + \frac{1}{4}\left(\left[\frac{\ell_p}{h}\right]^{4/3} + \tilde{f}\right)^{-1/2}, \tag{1}$$

where $\langle L \rangle$ is the average projected length of the chain measured along the tunnel and $\tilde{f} = f\ell_p/(k_B T)$ is the value of the force in its natural units $k_B T/\ell_p = 0.06$ pN. Note that $1 - \langle L \rangle/S = \langle m \rangle/(1 + \langle m \rangle)$. At zero force, one gets $0.1 < \langle m \rangle < 0.5$, for $2 \times 10^{-4} < n < 4 \times 10^{-2}$. Clearly, the excess length stored in the thermal fluctuations cannot account for excess length values up to $\langle m \rangle = 4$ as observed from the experiments; see Fig. 3. This implies that the actual confining tunnel follows a longer wiggled suboptical primitive path.

The shape of the primitive path is determined by the pinning process occurring at the adhesive front; it thus reflects the conformation of the DNA chains at the junction between the tunnel under formation and the free coil head. The spreading process, through a combination of hydrodynamic stresses and direct membrane-DNA interactions, applies a force to the coiled head that induces the average stretching state captured by the stapling mechanism. The relevant force extension relationship does not depend, in this case, on the confinement. An interpolation formula that accounts both for the strong stretching regime described by the limit of zero confinement in Eq. (1) and for the weak stretching limit where the extension is determined by the linear response of the fluctuating coil can be written as [4]

$$\tilde{f} = \frac{\langle z \rangle}{S} - \frac{1}{4} + \frac{1}{4(1 - \langle z \rangle/S)^2}, \tag{2}$$

where $\langle z \rangle$ is the average projected length. Using Eq. (2) with $\langle m \rangle = S/\langle z \rangle - 1$ gives force values in the range $0.85 < \tilde{f} < 15$ for the tadpole conformations and $0.35 < \tilde{f} < 1.3$ for the tapeworms. Note that forces of order $\tilde{f} \simeq 1$ or $f \simeq k_B T/\ell_p = 0.06$ pN are expected from the entropic repulsion between a wall and a polymer; larger forces must be related to different effects like the hydrodynamic stresses generated by the strong shear region in the immediate vicinity of the advancing front. Estimates based on the observed maximum velocity $v = 10\ \mu\mathrm{m\,s^{-1}}$ [1] and a gap height h of order of 10 nm lead to a shear rate $\dot{\gamma} = v/h \sim 10^3\ \mathrm{s^{-1}}$ which can easily account for the highest observed stretching values. However, observed spreading processes are smooth; the velocity measured from the

spreading front decreases linearly from the initial nucleation site to the final maximum adhesion patch radius. The measured differences of stretching behavior between the tapeworms and the tadpoles can thus only be accounted for by additional friction sources. We argue in the following that they are caused by internal friction forces related to self-entanglements.

We consider here a self-entanglement of the DNA, meaning a configuration of the chain that acts like a gate [5,6] through which the unwinding coil needs be threaded. In the absence of self-entanglements, the scraping mechanisms can only induce a modification of the chain configuration from a coil to an open, extended shape, if the largest time for chain relaxation is smaller than the characteristic time of vesicle spreading. For a coil of radius $R \sim 1$ μm and water viscosity $\eta = 10^{-3}$ Pa $\cdot$ s, the associated friction ζ is given by the Stokes friction $\zeta \sim \eta R$, and the longest Zimm relaxation time is $\tau_Z \sim R^2\zeta/(k_BT) = \eta R^3/(k_BT) = 0.2$ s, smaller than the vesicle spreading time $\tau_S \sim 10$ s. In the presence of p self-entanglements, the chain relaxation time can be simply estimated from p and ζ_1, the local friction in a gate due to local contacts, ζ_1 being arguably higher than hydrodynamic friction. For the experimental conditions described here the DNA chain can be pictured as a Gaussian chain with $N = S/\ell_p \sim 300$ monomers of size ℓ_p. Thus considering Gaussian statistics, the averaged number of self-entanglements p, involving monomers distant along the chain, is expected to be given by $p = \sqrt{S/\ell_p}$, and the number of monomers M in a polymer strand between two gates by $M = N/p = \sqrt{S/\ell_p}$. The friction from one gate ζ_g is therefore $\zeta_g = \sqrt{M}\zeta_1$, and the total friction estimated by this model reads $\zeta = p\zeta_g = (S/l_p)^{3/4}\zeta_1$. As a consequence, the time τ_E it takes the chain to relax self-entanglements is $\tau_E \sim N^{11/4}$, larger by at least 3 orders of magnitude than the Zimm time estimated above, $\tau_Z \sim N^{3/2}$.

The fundamental differences in our experiments between tadpole and tapeworm configurations, observed under the same vesicle, can be fully understood by invoking such long self-entanglement relaxations. Upon scraping, a chain with no self-entanglements in the polymer section that undergoes unwinding can be pushed to the border of the adhesive patch in a smooth manner, leading to a tadpole configuration. If the spreading membrane comes across one self-entanglement during the scraping process, it will locally stretch the chain but eventually will roll over it leaving behind the excess of chain contour length that was not able to unwind. This corresponds to the tapeworms' configurations that are confined below the adhesion patch and display large stretching fluctuations. Note that heterogeneities in the spatial distribution of the binders cannot account for the observed stretching variations.

The existence of self-entanglements in polymers has been theoretically conjectured for more than two decades within the framework of renormalization group theory, from the statistics of contacts between two Gaussian chains [7] and of mutual entanglements [8,9]. In spite of the importance of self-entanglements for understanding polymer chain dynamics, these theories have never been put to the test because of the intrinsic difficulty of demonstrating the presence of such chain configurations [10]. We have shown here that the scraping and stapling of an end-grafted DNA chain by the spreading front of a bioadhesive vesicle provide a unique experimental geometry sensitive to long relaxation processes as those expected from self-entanglements. Further efforts for better quantifying the forces acting on the DNA chains during scraping are currently undertaken in the Strasbourg group where preliminary results from the analysis of spread configurations of double-end-grafted DNA molecules not only confirm friction heterogeneity but also allow for an absolute calibration of the force values.

We thank the French Ministère de la Recherche, the Université Pierre et Marie Curie–Paris 6, Ville de Paris, and the Centre National de la Recherche Scientifique for financial support. G. N., A. J., N. L., F. T., and C. M. benefited from the STAR program. Y. S. acknowledges support from the Soft Condensed Matter IRTG. This work is also supported by a Korea Research Foundation Grant funded by the Korea government (MOEHRD, Basic Research Promotion Fund) (KRF 2008-531-C00030) (N.-K. L.).

*carlos.marques@ics-cnrs.unistra.fr
†lee@sejong.ac.kr

[1] M. L. Hisette, P. Haddad, T. Gisler, C. M. Marques, and A. P. Schroder, Soft Matter **4**, 828 (2008).
[2] D. Cuvelier and P. Nassoy, Phys. Rev. Lett. **93**, 228101 (2004).
[3] We excluded configurations when the total intensity was considerably different from the most probable value ($\sim$15%), thus avoiding error sources related to unusual DNA segments such as broken ones.
[4] J. F. Marko and E. D. Siggia, Macromolecules **28**, 8759 (1995).
[5] N.-K. Lee and S. P. Obukhov, J. Phys. II (France) **6**, 195 (1996).
[6] N.-K. Lee, C. Abrams, A. Johner, and S. P. Obukhov, Phys. Rev. Lett. **90**, 225504 (2003).
[7] B. Duplantier, Commun. Math. Phys. **117**, 279 (1988).
[8] A. N. Semenov, J. Phys. (Orsay, Fr.) **49**, 175 (1988); **49**, 1353 (1988).
[9] The exponent Z is defined from $\tau_E \sim N^Z$. While our simple argument suggests $Z = 11/4$, the more sophisticated calculations lead to $Z \approx 3$. There is a finite probability P_0 for two half-chains not to intersect at all $P_0 \propto N^{-5/16}$ (to second order in $\epsilon = 4 - d$) [7].
[10] M. Adam and M. Delsanti, J. Phys. (Orsay, Fr.) **45**, 1513 (1984).